# MAGNETISM: A SUPRAMOLECULAR FUNCTION

S. DECURTINS, R. PELLAUX, H.W. SCHMALLE
Institut für Anorganische Chemie, Universität Zürich,
Winterthurerstrasse 190, CH-8057 Zürich, Switzerland

and

P. FISCHER
Laboratorium für Neutronenstreuung, ETH/PSI
CH-5232 Villigen PSI, Switzerland

ABSTRACT

The field of molecule-based magnetism has developed tremendously in the last few years. Two different extended molecular — hence supramolecular — systems are presented. The Prussian-blue analogues show some of the highest magnetic ordering temperature of any class of molecular magnets, $T_C$ = 315 K, whereas the class of transition-metal oxalate-bridged compounds exhibit a diversity of magnetic phenomena. Especially for the latter compounds, the elastic neutron scattering technique has successfully been proven to trace the magnetic structure of these supramolecular and chiral compounds.

## 1. Introduction

Why should chemists become enthusiastic about magnetism ? Isn't it that the world of "real" magnets, dominated by physics and material science, goes on in its preoccupation with metals, objects that are opaque, shiny, and go clang when they hit the floor. These materials do not overlap much with the kind of compounds that chemists make in their flasks and beakers. Furthermore, the information-storage industry relies heavily on transition-metal oxides, whether simple binary ones like $\gamma$-$Fe_2O_3$ and $CrO_2$ or complex solid solutions based on the garnet or ferrite structures. Given that so many conventional magnetic materials are available with Curie temperatures far above room-temperature, not to mention high coercive and remanent fields, it is worth asking why much effort should being devoted to the synthesis of so called molecule-based magnetic materials.

All these points in question which are taken from a short perspective, entitled "The Chemistry of Magnets", and written by Peter Day, should call the reader's attention to this novel and exciting research field of molecular magnetism [1].

When did the research activities in the area of molecule-based magnetism start ? The first genuine molecular compound displaying a ferromagnetic transition was described by Wickman et al. as early as 1967 [2]. This compound, a chlorobis(diethyldithio-carbamato)iron(III), exhibiting an intermediate spin S = 3/2, orders ferromagnetically at 2.46 K. Since then, over the years, a scientific community has been established throughout the world focusing on the aspects of molecular magnetism and an increasing

number of international conferences have turned up a lot of new chemistry and brought synthetic chemists into close contact with physics and material science. Especially since 1989, there have been five International Conferences on Molecule-Based Magnets organized in the United States, in Japan, and in Europe, which demonstrates that the study of the magnetic properties of molecule-based materials has become an important focus of scientific interest [3,4].

There are several features of potential practical impact that distinguish magnetic materials based on molecules from their analogues consisting of continuous ionic or metallic lattices. Examples would include the search for materials combining two- or more functional properties, e.g. magnetism and transparency for magneto-optical applications or the design of mesoscopic molecules possessing large magnetic moments. Synthetic methods will also be quite different and consequently, magnetic thin films might be deposited with methods such as solvent evaporation.

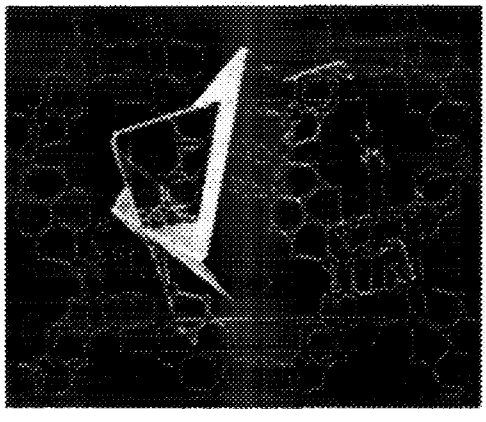

Fig. 1: Chemistry is moving from molecular magnetochemistry to solid state supramolecular magnetochemistry. Single crystal of a chiral 3D network compound with transition-metal ions as spin carriers [22].

A brief comment of the characteristics of the elements that constitute a magnetic molecular solid will give us a feeling of the extension, complexity and wide diversity of magnetic phenomena that can be found in these materials. A magnetic molecular solid can be formed by free radicals, transition-metal ions, rare earth ions and diamagnetic ligands. Any combination of these components is possible although only the free radicals can form a magnetic molecular solid by themselves. In the following, we will concentrate only on coordination compounds, where the importance of transition-metal ions as spin carrier centers stems at least from three main reasons: i) transition-metal to ligand interactions are extremely variable, thus the building up of novel, higher-dimensional architectures can profit very much from the coordination algorithm of the metal ions as well as from the availability of various bridging ligand systems; ii) transition-metals are prone to quick and reversible redox changes, hence supramolecular functions like energy- and charge-transfer processes can anticipate from it; iii) the collective features of components bearing free spins may result in supramolecular assemblies exhibiting molecule-based magnetic behavior, whereby the critical role of the dimensionality of the compounds is simultaneously taken into account. Accordingly, molecular precursors implying transition-metal ions entail the synthesis of ferro- and antiferromagnetic systems with a tuneable critical temperature.

To sum up, molecular magnetism is by essence of supramolecular nature. It results from the collective features of components bearing free spins and on their arrangement in organized assemblies. Accordingly, it is the supramolecular chemistry, the design of systems exhibiting molecular self-organization, which expresses the strategy of the

synthetic chemist of creating novel materials which combine a selected set of properties, for instance from the areas of photophysics, photochemistry, magnetism and electronics.

In the following, two different, supramolecular systems will be discussed. The Prussian-blue analogues reveal compelling results with respect to high critical temperature and tuneable magnetic phase transitions also with electronic and optical stimuli, whereas the supramolecular transition-metal oxalate systems have been chosen to demonstrate the possibilities of the elastic neutron scattering technique for elucidating the magnetic structures in extended two- and three-dimensional molecular systems.

## 2. The Prussian-Blue Analogues

The Prussian-blue analogues represent a cornerstone in the field of molecular magnetism. In fact, the latest striking example in the field of molecular magnetism is the Prussian-blue-like phase which has been reported in 1995 to behave as a magnet below a critical temperature of 315 K [5]. Fig. 2 depicts the thermal dependence of the magnetization of this organometallic magnet. That specific solid, as well as other analogues prepared from hexacyanometalate building blocks consistently show some of the highest magnetic ordering temperature of any class of molecular magnets. For example, compounds with stoichiometries $Cs_2Mn[V(CN)_6]$, $[NEt_4]_{0.5}Mn_{1.25}[V(CN)_5]\cdot 2H_2O$ and $V[Cr(CN)_6]_{0.86}\cdot 2.8H_2O$ exhibit magnetic ordering temperatures of 125 K, 230 K and 315 K respectively [5,6]. Typically and obviously when looking at the stoichiometries, these compounds have to be characterized as amorphous, non-stoichiometric solids. Therefore, Fig. 3 exhibits only an idealized unit cell of a three-dimensional cubic structure.

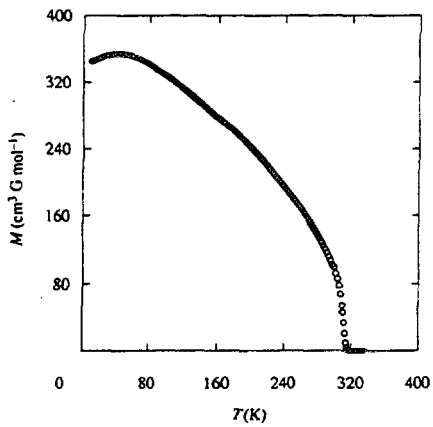


Fig. 2: Thermal dependence of the magnetization of the dark blue solid $V[Cr(CN)_6]_{0.86}\cdot 2.8H_2O$ in low applied field (H = 10 G) [5]. Note, that $T_C$ = 315 K.

Prussian-blue, a pigment obtained by the reaction of the diamagnetic $[Fe(CN)_6]^{4+}$ complex anion with the $Fe^{3+}$ cation is the first synthetic coordination compound to be reported already in 1710 [7]. It owes its name to the color of the deep blue precipitate of $Fe_4[Fe(CN)_6]_3\cdot 15H_2O$. Thereby, the intense absorption band at 700 nm is due to a transition from the ground state to an excited state in which an electron is transferred from an Fe(II) to an Fe(III) site, thus the compound may be considered as the archetype of mixed valence compounds, containing two identical metals in different oxidation states.

Prussian-blue's attraction for chemists and physicists lies not only in its optical properties but also in its magnetic properties. The compound shows a long-range magnetic ordering at $T_C$ = 5.6 K [8]. The critical temperature is low, because only the Fe(III) sites carry a spin, whereas the Fe(II) sites are diamagnetic. Therefore, the magnetic interaction

must occur between next-nearest ions through the 10.6 Å long Fe(III)-C-N-Fe(II)-N-C-Fe(III) linkages. The possibility of propagating magnetic interactions is due to the strong spin delocalization from the metal ions towards its nearest neighbors. The presence of strong spin densities on the nitrogen and carbon atoms of the cyano groups has been experimentally observed by polarized neutron diffraction [9].

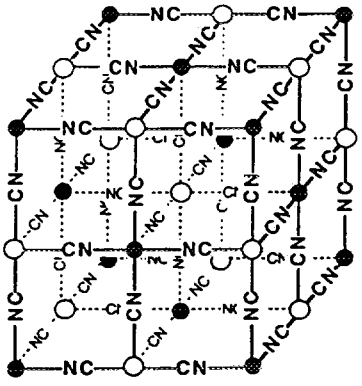

Fig. 3: Idealized unit cell of the three-dimensional, face-centered cubic structure: (•), (o) are different metal ions. Water molecules and interstitial ions in the unit cell were omitted for clarity.

The substitution of Fe(II) and Fe(III) by other ions A and B leads to a family of compounds with the rock salt structure. In these compounds, molecular hexacyanometalate anions $[B(CN)_6]^{p-}$ and the metallic cation $A^{q+}$ occupy alternate vertices of the cubes, where the A-N-C-B distance is about 5 Å. When paramagnetic ions are used, compounds with various magnetic properties are created. Babel was the first, in 1982, to reach a high Curie temperature of 90 K with a ferrimagnetic Cr(III)/Mn(II) system [10]. Since then, the Curie temperatures continued to increase by varying the A and B ions and finally 315 K is reached with a Cr(III)/[V(II)-V(III)] compound [5]. In that particular case, the V(II)-Cr(III) and V(III)-Cr(III) interactions are strongly antiferromagnetic, and the compound behaves as a ferrimagnet with a high critical temperature. In addition to the value of the critical temperature, the saturation magnetization and the coercivity are also important characteristics of a magnetic material. In the present case, the saturation magnetization is limited to 0.15 Bohr magnetons, owing to the weak value of the resulting spin per repeat unit. The coercivity is also weak: at 10 K, the value of the coercive field is only 10 Oe; at least 100 Oe would be needed to be useful in recording media.

Overall and most importantly, a room-temperature molecular magnet is realized and prospectively, molecular electronics may emerge from such kind of molecular magnets. Only recently, Hashimoto et al. reported the synthesis of molecule-based ferrimagnetic thin films with high critical temperatures by means of a simple electrochemical route [11]. The compounds are mixed-valence chromium cyanides, for example $[Cr^{II}_{0.36}Cr^{III}_{1.76}(CN)_6] \cdot 2.8H_2O$ for $T_C$ = 270 K, and their magnetic phase transitions could be controlled electrochemically after the film preparation. Fig. 4 demonstrates that these materials can be switched from ferrimagnetism or paramagnetism, e.g. between 100 K and 240 K depending on the stoichiometry.

In addition to the electrochemical tuning of molecule-based magnets, another possibility is the induction of a magnetic phase transition by optical stimuli. This effect was demonstrated with the report of a photoinduced magnetization change observed in a cobalt-iron cyanide [12]. Fig. 5 illustrates this effect with the field-cooled magnetization versus temperature curves.

This concise report about the Prussian-blue analogues with their high critical temperatures and tuneable magnetic phase transitions through electrical and optical stimuli demonstrates adequately the targets of the ongoing research in the field of molecule-based magnetic materials.

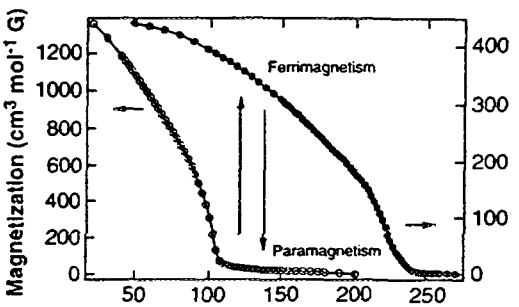


Fig. 4: Magnetic bistability induced by the redox reaction of Cr(III) in the mixed-valence chromium cyanides. FCM versus temperature before (■) and after (□) electrochemical reduction [11].

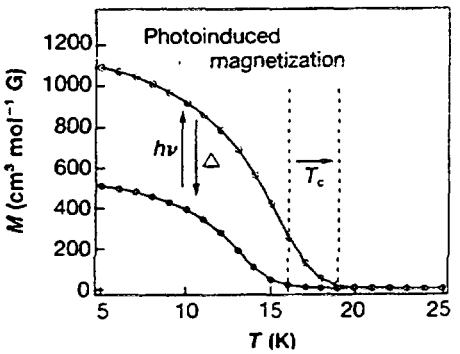


Fig. 5: FCM versus temperature curves at H = 5 G before (•) and after (o) red light irradiation of a cobalt-iron cyanide. The magnetization enhanced by illumination (hν) can be removed by thermal treatment (Δ) above 150 K [12].

## 3. The Supramolecular Transition-Metal Oxalate Compounds

### 3.1. The System

A successful molecular design of metal-complex magnets which are based on trioxalatochromium(III) building blocks (compare Fig. 6B), has been reported in 1992 [13]. Within a series of layered, oxalate-bridged bimetallic compounds, ferromagnetic ordering behavior has been shown to occur at temperatures < 14 K. Since then, a variety of analogous two-dimensional (2D), bimetallic assemblies, also with mixed-valency stoichiometries, have been prepared and characterized [14-20]. Overall, many of these layered compounds exhibit ferro-, ferri- or antiferromagnetic long-range ordering behavior and in some cases they show at least evidence for short-range interactions. Furthermore, as an extension to the structurally two-dimensional compounds, it seemed likely, that also three-dimensionally-bridged metal assemblies could be realised. Accordingly, on the basis of a chiral template, namely a tris-bipyridine transition-metal complex (compare Fig. 6A), three-dimensional (3D), homo- and heterometallic oxalate-bridged frameworks have been synthesized [21-23].

As expected, these supramolecular host/guest compounds reveal an interesting structural topology, and in addition, many of them show a long-range magnetic ordering behavior as well as various kinds of photophysical properties. Given that an astonishing diversity of magnetic phenomena is generated by these polymeric 2D and 3D framework compounds and that a large body of experimental results is reported from magnetic susceptibility and magnetization studies, very limited experience has been gained so far from elastic neutron scattering experiments aimed at elucidating the spin structure in the magnetically ordered state. Therefore, we focus on some results of neutron scattering experiments with the 2D and 3D oxalate-bridged transition-metal compounds [20,23].

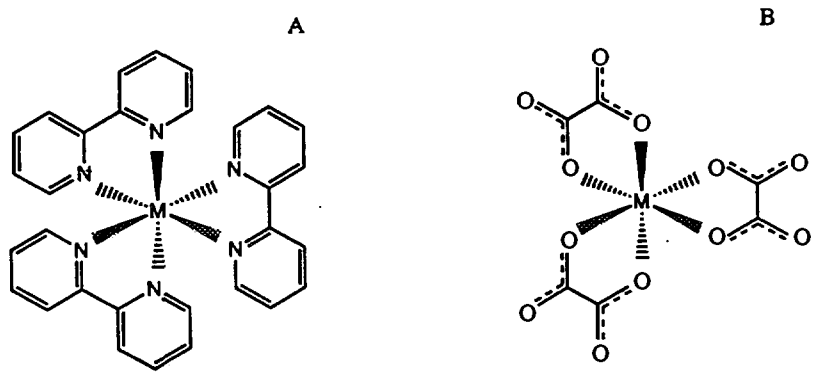


Fig. 6: Schematic representations of the two chiral (the Λ-isomers are shown) preorganized cationic (A) and anionic (B) coordination entities. M = transition-metal ion as spin carrier center.

In addition, an overview about possible photophysical processes occurring in the 3D supramolecular host/guest compounds is presented. Thereby, we address the basic idea in the field of molecular magnetism, namely to engineer novel molecular compounds that are not only magnetic but which also possess additional characteristics, for instance in the field of photophysics [22,25].

## 3.2. Basic Structural Principles

The oxalate ion, $C_2O_4^{2-}$, is well known to be an attractive ligand, because its ambidentate coordinating ability enables the construction of homo- and bimetallic chain- and layer-structures, and even the formation of three-dimensionally connected transition-metal frameworks. In the following, we will discuss some basic ideas which are relevant for the understanding of the two- and three-dimensional framework topologies. Both structure types are formally composed of $[M^{z+}(ox)_3]^{(6-z)-}$ building blocks, whereby each of these units represents a three-connected point. These subunits which are predestined to create extended network motifs, may polymerise in principle in two ways. Thereby, one alternative leads to a 2D honeycomb layer compound, whereas in the other possible arrangement, an infinite 3D structure is formed. In the former case, building blocks of different chirality are alternately linked and consequently, the bridged metal ions are confined to lie within a plane, as it is illustrated in Fig. 7a. Consequently, a layered structure motif will result. In contrast, as it is depicted in Fig. 7b, an assembling of building blocks of the same chiral configuration will lead to a 3D framework structure.

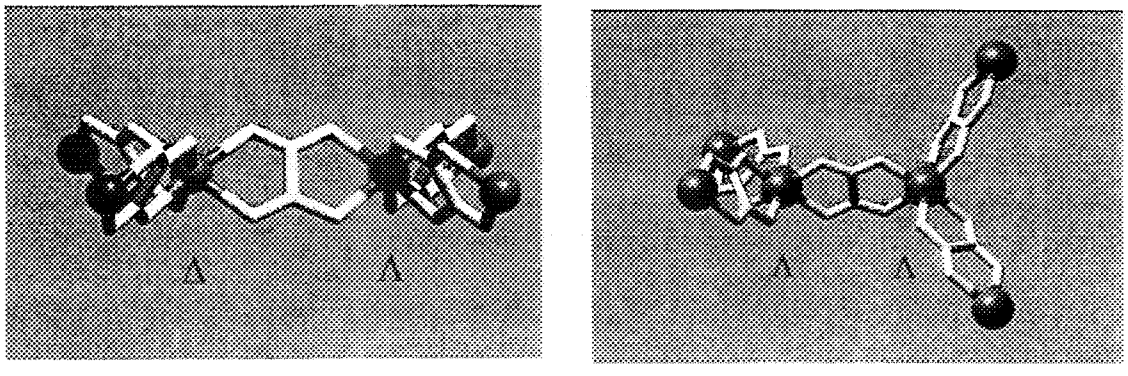


a b

Fig. 7: Chiral $[M^{z+}(ox)_3]^{(6-z)-}$ building blocks assembled with a) alternating chiral configuration, b) equal chiral configuration.

As a next step, simple topological rules will be applied in order to define the number of subunits which are needed to build closed circuits, hence, extended framework motifs. Fig. 8 illustrates the way that two dimeric subunits may be combined to form the planar honeycomb network. In an analogous manner, it can easily be seen from Fig. 9, that two tetrameric subunits are needed to build closed circuits composed of ten metal centers, which in sum define the three-dimensional decagon framework structures.

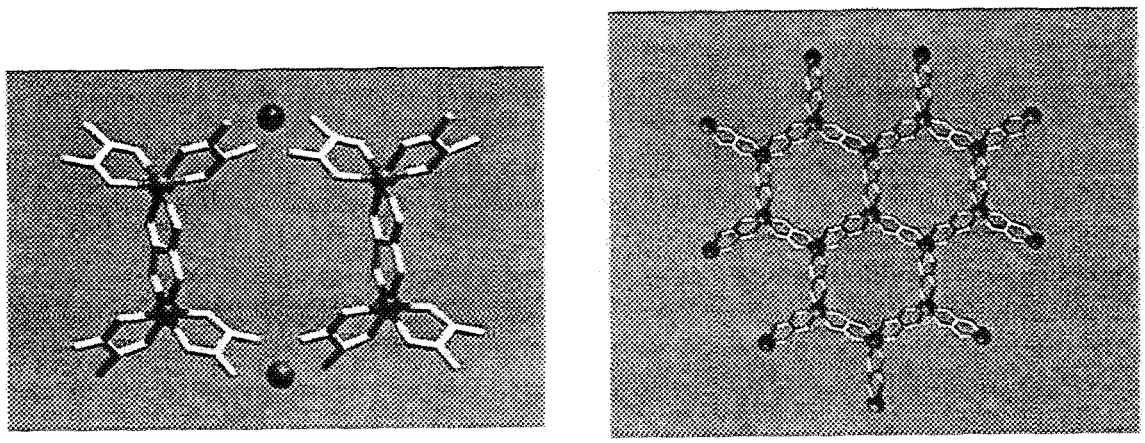

a b

Fig. 8: a) Two dimeric units of the alternating chirality type are necessary to form a closed hexagon ring; b) the resulting planar network motif.

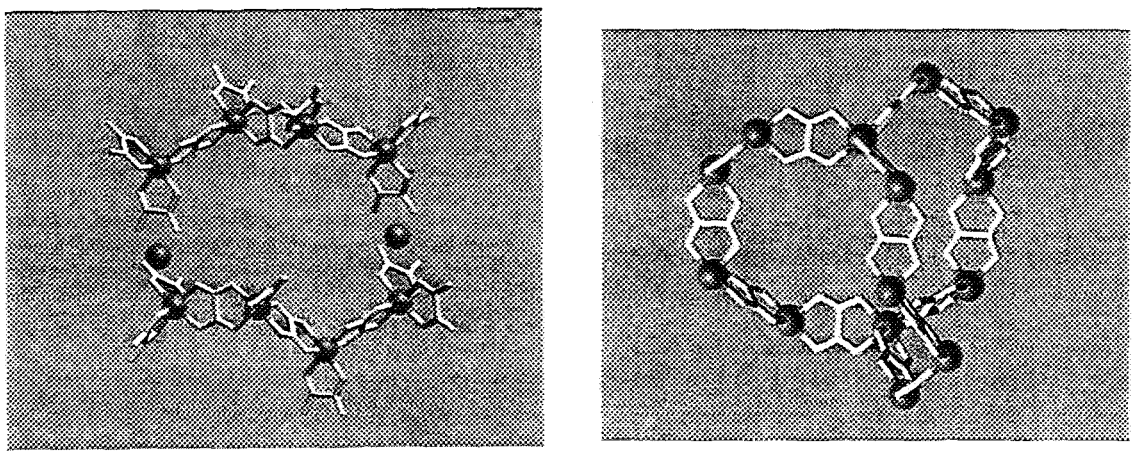

a b

Fig. 9: a) Two tetrameric units of the same chirality type are necessary to form a closed decagon ring; b) a fragment of the 3D, chiral framework.

### 3.3. The Honeycomb Layer Structure

The discrimination between the formation and crystallization either of a 2D or a 3D framework structure relies on the choice of the templating counterion. Evidently, the template cation determines the crystal chemistry. In particular, $[XR_4]^+$ (X = N, P; R = phenyl, n-propyl, n-butyl, n-pentyl) cations initiate the growth of 2D layer structures containing $[M^{II}M^{III}(ox)_3]_n^{n-}$, $M^{II}$ = V, Cr, Mn, Fe, Co, Ni, Cu, Zn; $M^{III}$ = V, Cr, Fe, network stoichiometries. The structures consist of anionic, 2D, honeycomb networks which are interleaved by the templating cations. Although these 2D compounds are not chiral, they express a structural polarity due to the specific arrangement of the templating

cations (see Fig. 10). These organic cations which are located between the anionic layers, determine the interlayer separations. From single-crystal X-ray studies, these distances have been determined to the values 9.94 Å, 9.55 Å, 8.91 Å, and 8.20 Å for the n-pentyl, phenyl, n-butyl, and n-propyl derivatives [14,15,18,20].

### 3.4. The Chiral 3D Structure

The cationic, tris-chelated transition-metal diimine complexes, $[M(bpy)_3]^{2+/3+}$, act as templates for the formation and crystallization of the 3D decagon framework structures [21-23]. As outlined above, the topological principle implies for the 3D case, that only subunits of the same chiral configuration are assembled. Consequently, the uniform anionic 3D network-type with stoichiometries like $[M^{II}_2(ox)_3]_n^{2n-}$, $[M^{I}M^{III}(ox)_3]_n^{2n-}$ or $[M^{II}M^{III}(ox)_3]_n^{n-}$ is chiral, as it is composed of 2n centers exhibiting the same kind of chirality. Naturally, this chiral topology is in line with the symmetry elements which are present in the crystalline state of the 3D frameworks, which in sum constitute either one of the enantiomorphic cubic space groups P4332 or $P4_132$ for the former and the cubic space group $P2_13$ for the latter bimetallic stoichiometries. Thereby, the 2n metal ions occupy special sites with a three-fold symmetry axis. Fig. 11 depicts a stereo view of the decagon network topology.

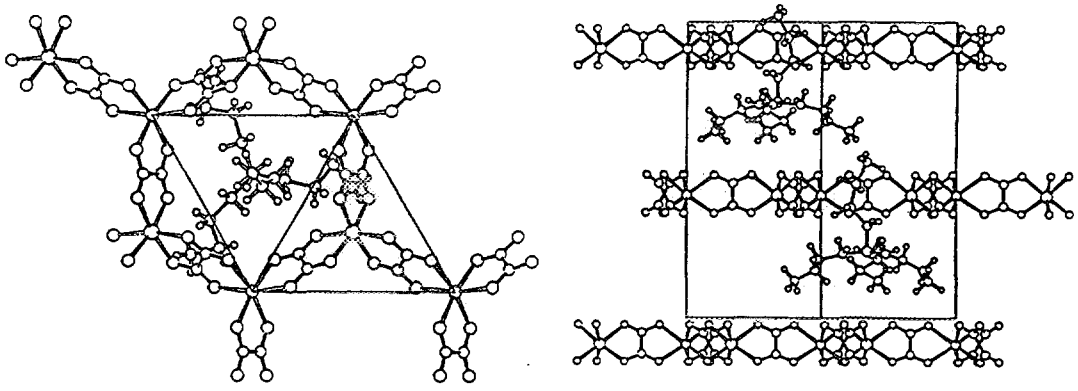

a b

Fig. 10: Sector from the $[N(n\text{-butyl})_4][Mn^{II}Fe^{III}(ox)_3]$ layer compound. a) [001] projection; b) [110] projection [20].

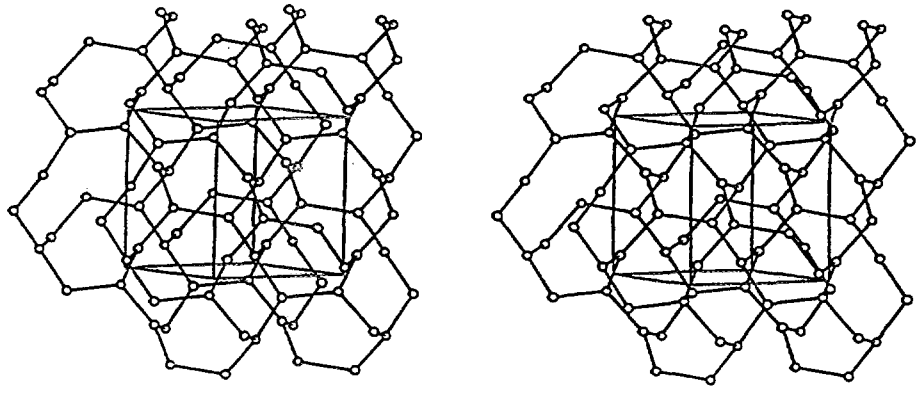

Fig 11: Stereo view of the 3-connected 10-gon (10,3) network topology.

3.5. Magnetic Structure of a 2D Ferromagnet

The layer compound with stoichiometry $[A][Mn^{II}Cr^{III}(ox)_3]$, is known to exhibit a transition to a ferromagnetically ordered state at $T_C$ = 6 K [13-15,20]. A single-crystal field-dependent magnetization experiment with the compound $[N(n\text{-propyl})_4][Mn^{II}Cr^{III}(ox)_3]$, revealed a distinct anisotropic behavior such that the easy-axis of magnetization is lying predominantly in the direction of the c-axis, thus perpendicular to the hexagonal network [20]. As it is illustrated in Fig. 12, with the parallel orientation of the external field to the c-axis, the saturation is reached in a field of H ≈ 0.1 T, while the saturation field in the perpendicular direction is H > 0.3 T. This finding is in accordance with the results of the neutron scattering experiments (vide infra).

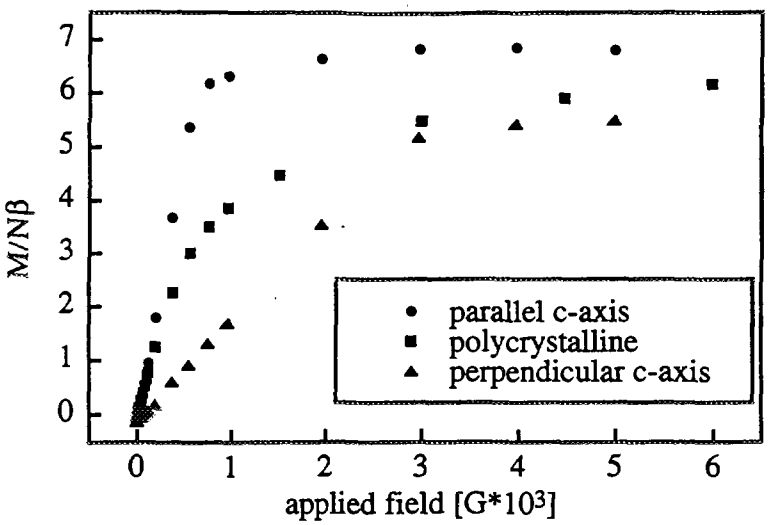


Fig. 12: Plot of the field dependence of the magnetization for a single-crystal of $[N(n\text{-propyl})_4][Mn^{II}Cr^{III}(ox)_3]$ at T = 4.2 K [20].

In order to verify the magnetic long-range ordering character below $T_C$ = 6 K, and to elucidate experimentally the magnetic structure of that ferromagnetic compound, an elastic neutron scattering study was undertaken with a polycrystalline sample with $A^+ = [P(C_6D_5)_4]^+$ [20]. First, the structural part of the diffraction pattern had to be examined from room-temperature down to liquid-helium temperatures. Fig. 13 shows a profile matching of a 1.8 K neutron diffraction pattern of the polycrystalline sample. The refined unit cell parameters within space group R32 show the values a=b=18.749(3) Å, c=111.89(3) Å. The c-axis was formerly determined from a single-crystal X-ray measurement at room-temperature within space group R3c to a value of c=57.283(24) Å [15]. The doubling of the c-axis as a result from the refinement of the neutron diffraction pattern, is interpreted to originate either from a superstructure phenomenon or from a twinning effect.

Furthermore, as anticipated from the magnetic susceptibility data, a difference in the peak intensities due to long-range ferromagnetic ordering of the magnetic moments from the $Mn^{2+}$ and $Cr^{3+}$ ions could be detected from the neutron diffraction experiment at the temperatures 1.8 K and 12 K. Fig. 14 illustrates the observed [difference I(1.8 K) - I(12 K)] and calculated magnetic neutron diffraction patterns. Thereby it has to be noted, that the increase of the intensities corresponds to a propagation vector **k** = 0. The temperature dependence of the dominant magnetic intensity at $2\Theta$ = 69,1° indicates an ordering

temperature of 6.0(5) K, in good agreement with the magnetic susceptibility measurements. The observed enhancement in some of the Bragg reflections proves the presence of long-range magnetic interactions within this structurally two-dimensional compound. Finally, the best agreement between observed and calculated neutron intensities was achieved with a collinear ferromagnetic arrangement of both the $Mn^{2+}$ and $Cr^{3+}$ spins along the c-axis.

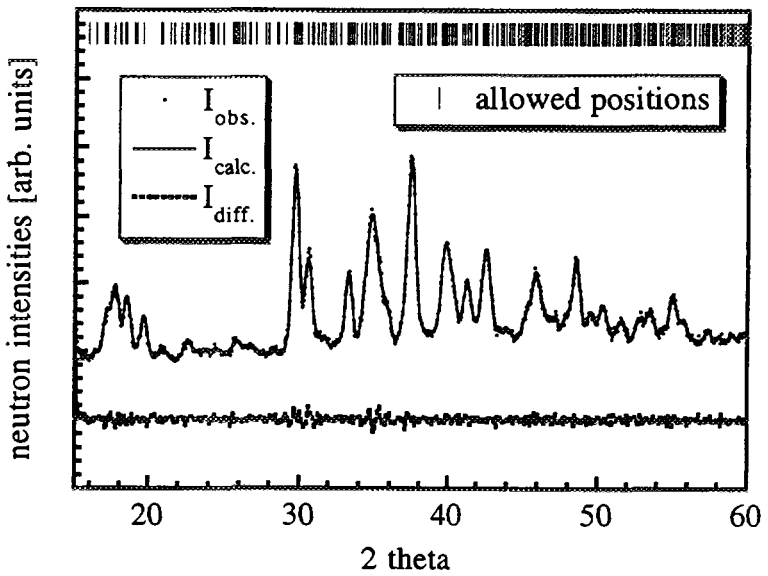


Fig. 13: Observed neutron diffraction pattern of a polycrystalline sample of $[P(C_6D_5)_4][Mn^{II}Cr^{III}(ox)_3]$ at T = 1.8 K with the profile matching plot for space group R32. $\lambda$ = 2.398 Å [20].

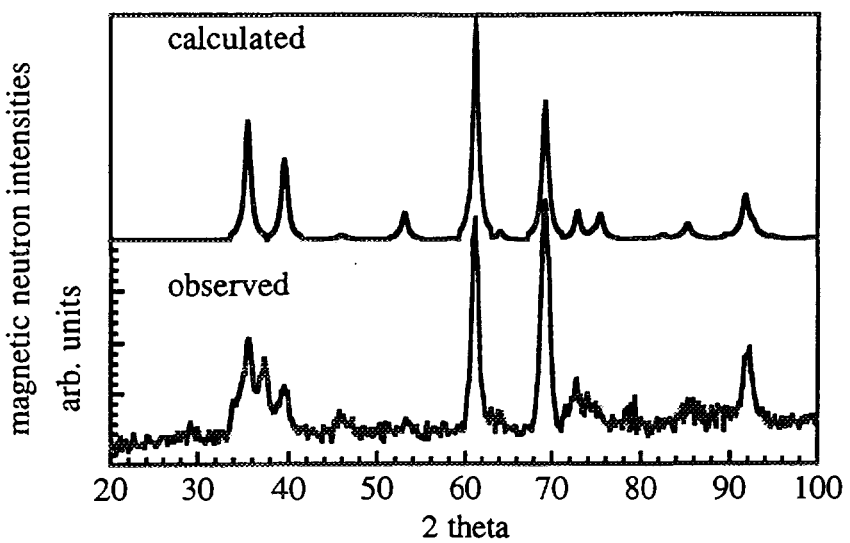


Fig. 14: Observed [difference I(1.8 K) - I(12 K)] and calculated magnetic neutron diffraction patterns of a polycrystalline sample of $[P(C_6D_5)_4]$ $[Mn^{II}Cr^{III}(ox)_3]$; $\lambda$ = 4.766 Å. The calculation is based on a ferromagnetic spin configuration parallel to the c-axis [20].

### 3.6. Magnetic Structure of a 3D Antiferromagnet

The existence of a magnetically ordered phase for the compound $[Fe(bpy)_3][Mn^{II}_2(ox)_3]$ could be deduced from magnetic susceptibility measurements,

which revealed a rounded maximum at about 20 K in the $\chi_M$ versus T curve (thus $T_N$ < 20 K) as well as a Weiss constant $\Theta$ of -33 K in the $1/\chi_M$ versus T plot [21]. As anticipated, an increase of the intensities due to long-range antiferromagnetic ordering of the spins from the $Mn^{2+}$ ions could be detected with the neutron diffraction experiments performed in the temperature range from 30 K to 1.8 K with a deuterated polycrystalline sample [23]. Fig. 15 illustrates the observed [difference I(1.8 K) - I(30 K)], calculated and difference magnetic neutron diffraction patterns. The increase of the intensities corresponds to a propagation vector **k** = 0, thus the magnetic unit cell is equal to the chemical cell.

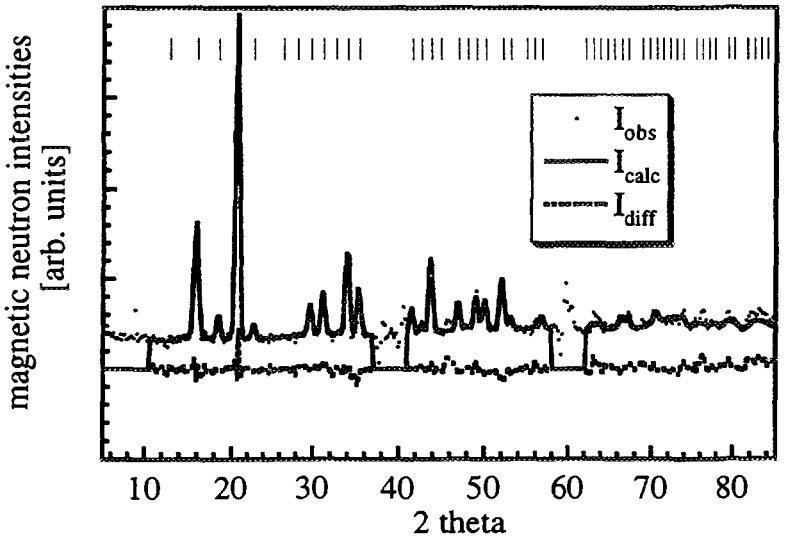


Fig. 15: Observed [difference I(1.8 K) - I(30 K)], calculated and difference magnetic neutron diffraction patterns of a polycrystalline sample of $[Fe^{II}(d_8\text{-bpy})_3][Mn^{II}_2(ox)_3]$; $\lambda$ = 2.5154 Å [23].

The best agreement between observed and calculated magnetic neutron intensities was achieved with a collinear, antiferromagnetic arrangement of the $Mn^{2+}$ moments according to the three-dimensional irreducible representation $\tau_4$, which is derived from the enantiomorphic pair of the chiral, cubic crystallographic space groups $P4_332$ / $P4_132$ [24]. Thus a two-sublattice spin configuration has been proven to occur. Naturally, in the present experiment, no information about a preferred direction of the magnetic moments with respect to the crystallographic axes can be gained from the polycrystalline sample with cubic symmetry. Fig. 16 depicts the pattern of the magnetic structure within the 3D manganese(II) network.

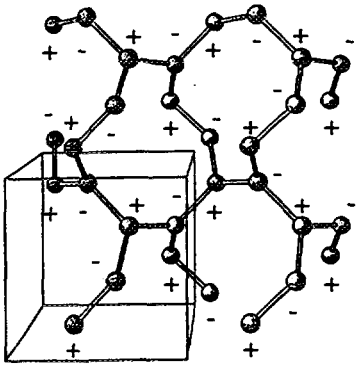

Fig. 16: A scheme of the AF, collinear configuration of the magnetic moments originating from the $Mn^{2+}$ ions, which constitute the chiral 3D network compound [23].

3.7. A Short Comment on Photophysical Properties

Chemical variation and combination of metal ions of different valencies in the oxalate backbone of the two- and three-dimensionally bridged frameworks as well as in the tris-bipyridine cations offer unique opportunities for studying a large variety of photophysical processes, such as light-induced electron transfer and excitation energy transfer in the solid state [22,25]. In this report we will comment on some observations of the excitation energy transfer processes within the 3D, supramolecular host/guest compounds. Depending upon the relative energies of the excited states of the chromophores, energy transfer is observed either from the guest system with the tris-bipyridine cations as donors to the host system where the oxalate-backbone acts as acceptor sites or vice versa. In addition, energy migration, that is excitation energy transfer between identical chromophores, occurs within the host as well as within the guest system [25]. The following stoichiometries $[Ru_{1-x}Os_x(bpy)_3][NaAl(ox)_3]$ and $[Ru(bpy)_3][NaAl_{1-x}Cr_x(ox)_3]$ are chosen to illustrate with examples these specific photophysical properties.

Fig. 17 shows the luminescence spectra of three representative compounds. If $Al^{3+}$ is replaced by $Cr^{3+}$, the $[Ru(bpy)_3]^{2+}$ luminescence from the spin-forbidden MLCT transition is completely quenched and the sharp luminescence bands characteristic for the zero-field components of the $^2E \longrightarrow {}^4A_2$ transition of octahedrally coordinated and trigonally distorted $Cr^{3+}$ are observed at 14'400 $cm^{-1}$.This is a clear indication for very efficient energy transfer from the initially excited $[Ru(bpy)_3]^{2+}$ to $[Cr(ox)_3]^{3-}$.

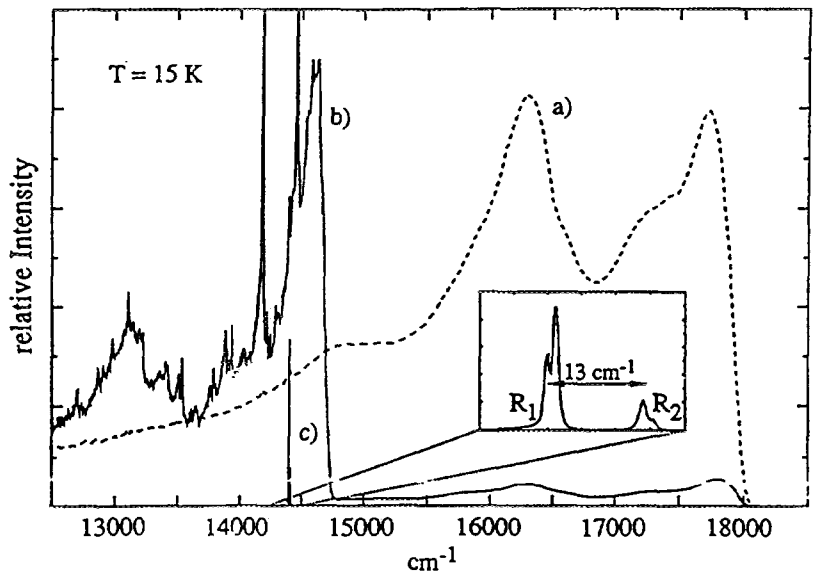


Fig. 17: Luminescence spectra at T = 15 K of a) $[Ru(bpy)_3][NaAl(ox)_3]$; b) $[Ru_{1-x}Os_x(bpy)_3][NaAl(ox)_3]$, x=1 %; c) $[Ru(bpy)_3][NaCr(ox)_3]$; $\lambda$=476 nm.

Not only acceptors on the oxalate backbone may quench the $[Ru(bpy)_3]^{2+}$ luminescence. Replacing a fraction of the $[Ru(bpy)_3]^{2+}$ by $[Os(bpy)_3]^{2+}$ results in luminescence from $[Os(bpy)_3]^{2+}$ and a quenching of the $[Ru(bpy)_3]^{2+}$ luminescence, too. Indeed, the energy transfer to $[Os(bpy)_3]^{2+}$ is even more efficient than to $[Cr(ox)_3]^{3-}$. This is due to the higher oscillator strength of the MLCT absorption on $[Os(bpy)_3]^{2+}$ as compared to the spin allowed d-d transition on $[Cr(ox)_3]^{3-}$. Fig. 18 summarizes within a schematic representation these different photophysical processes.

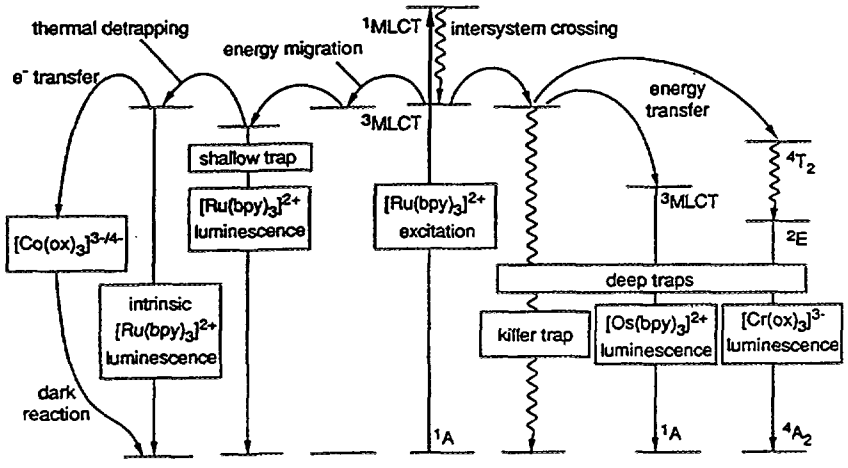


Fig. 18: Schematic representation of different photophysical processes observed in $[Ru_{1-x}Os_x(bpy)_3][NaAl(ox)_3]$ and $[Ru(bpy)_3][NaAl_{1-x}Cr_x(ox)_3]$.

## 4. Conclusions and Perspectives

Molecular magnetism is a new field of research which has emerged over the past decade or so. The heart of the field concerns the design and synthesis of molecular assemblies that show bulk properties such as long-range magnetic ordering combined with an additional supramolecular function, for example in the field of photophysics. The outlined results of the neutron diffraction experiments on the supramolecular transition-metal oxalate compounds have successfully proven to trace the spin configuration defining the antiferro- and ferromagnetic phases in a 3D and 2D molecular framework compound. The short comment on the photophysical energy-transfer processes within the 3D compounds points to another exciting aspect in the study of molecule-based magnetic materials.

The V International Conference on Molecule-Based Magnets, convened in July 1996 in Osaka, Japan, focused upon several key aspects that directly relate to the design, preparation, and physical study of molecule/polymer based magnets and high spin molecule/polymer systems. The VI International Conference is already announced for 1998 to be hosted in France. The field indeed is now a thriving branch of interdisciplinary science.

## 5. References

1. P. Day, *Science* **261** (1993) 431.
2. H.H. Wickman, A.M. Trozzolo, H.J. Williams, G.W. Hull, and F.R. Merritt, *Phys. Rev.* **155** (1967) 563.

3. Proceedings of the IV International Symposium on Molecule-Based Magnets; J.S. Miller, A.J. Epstein, Eds.; *Mol. Cryst. Liq. Cryst.*, Sect. A **271-274** (Gordon & Breach, London, 1995).
4. O. Kahn, *Molecular Magnetism* (VCH, Weinheim, 1993).
5. S. Ferlay, T. Mallah, R. Ouahès, P. Veillet, and M. Verdaguer, *Nature* **378** (1995) 701.
6. W.R. Entley, and G.S. Girolami, *Science* **268** (1995) 397.
7. Misc. Berolinensia ad Incrementum Sci. **1** (Berlin, 1710) 337.
8. R.M. Bozorth, H.J. Williams, and D.E. Walsh, *Phys. Rev.* **103** (1956) 572.
9. B.N. Figgis, E.S. Kucharski, and M. Vrtis, *J. Am. Chem. Soc.* **115** (1993) 176.
10. W.D. Griebler, and D. Babel, *Z. Naturforsch.* **37b** (1982) 832.
11. O. Sato, T. Iyoda, A. Fujishima, and K. Hashimoto, *Science* **271** (1996) 49.
12. O. Sato, T. Iyoda, A. Fujishima, and K. Hashimoto, *Science* **272** (1996) 704.
13. H. Tamaki, Z.J. Zhong, N. Matsumoto, S. Kida, M. Koikawa, N. Achiwa, Y. Hashimoto, and H. Okawa, *J. Am. Chem. Soc.* **114** (1992) 6974.
14. L.O. Atovmyan, G.V. Shilov, R.N. Lyubovskaya, E.I. Zhilyaeva, N.S. Ovanesyan, S.I. Pirumova, and I.G. Gusakovskaya, *JETP Lett.* **58** (1993) 766.
15. S. Decurtins, H.W. Schmalle, H.R. Oswald, A. Linden, J. Ensling, P. Gütlich, and A. Hauser, *Inorg. Chim. Acta* **216** (1994) 65.
16. W.M. Reiff, J. Kreisz, L. Meda, and R.U. Kirss, *Mol. Cryst. Liq. Cryst.* **273** (1995) 181.
17. C. Mathonière, C.J. Nuttall, S.G. Carling, and P. Day, *Inorg. Chem.* **35** (1996) 1201.
18. S.G. Carling, C. Mathonière, P. Day, K.M.A. Malik, S.J. Coles, and M.B. Hursthouse, *J. Chem. Soc., Dalton Trans.* (1996) 1839.
19. A. Bhattacharjee, S. Iijima, and F. Mitzutani, *J. Magn. Magn. Mater.* **153** (1996) 235.
20. R. Pellaux, H.W. Schmalle, R. Huber, P. Fischer, T. Hauss, and S. Decurtins, *Inorg. Chem.*, submitted.
21. S. Decurtins, H.W. Schmalle, P. Schneuwly, J. Ensling, and P. Gütlich, *J. Am. Chem. Soc.* **116** (1994) 9521.
22. S. Decurtins, H.W. Schmalle, R. Pellaux, P. Schneuwly, and A. Hauser, *Inorg. Chem.* **35** (1996) 1451.
23. S. Decurtins, H.W. Schmalle, R. Pellaux, R. Huber, P. Fischer, and B. Ouladdiaf, *Adv. Mater.*, in press.
24. O.V. Kovalev, *Representations of the Crystallographic Space Groups* (Gordon & Breach, Reading, 1993).
25. M.E. von Arx, A. Hauser, H. Riesen, R. Pellaux, and S. Decurtins, *Phys. Rev. B*, submitted.